Effects of Welding Sequence on Welding Deformation of Steel Q345D Based on Numerical Simulation with PAM-ASSEMBLY

Xueyong CHEN; Yifeng XIAO; Yi LI; Xiangwen LI
School of Mechanical Engineering, Xiangtan University, Xiangtan, China
1025835362@qq.com; sanyxyf@163.com; 53985966@qq.com; lixiangwen284@163.com

Abstract: Using the welding assembly finite element software, PAM-ASSEMBLY, we performed a dynamic simulation of Q345D low alloy high strength steel deformation under different welding sequences. A post processing module was used to gain welding deformation nephograms at different times under different welding sequences. The welding sequence of program 5 reduced the welding deformation by 11.95% compared to program 2, which suggests that reasonable arrangement and assemblage of welding sequence can effectively reduce welding deformation. The welding sequence of program 5 resulted in the smallest amount of welding deformation, which suggests that simultaneous welding during actual production is optimal. The results may serve as a guide for actual production and provide a reference to ultimately improve the weld-ability of Q345D low alloy high strength steel.

Keywords-PAM-ASSEMBLY; Q345; numerical simulation; welding sequence; welding deformation.

I. INTRODUCTION

The welding process is a special electric arc heating and cooling process. During heating, the weld material and the material near the weld seam zone is compressed by thermal expansion, generating compressive plastic strain. During cooling, the material stretches because the surrounding area is cooler, rapidly reducing its temperature and generating tensile plastic strain. Because the tensile plastic strain cannot be completely offset by the compressive plastic strain, the structure will deform after welding, which will affect the normal assembly and use of the structure[1-3]. Thus, optimization of the welding sequence is crucial for control of welding deformation. The use of numerical techniques to simulate the welding process is not new and the increase in computing power has seen the size and complexity of the models increase.

For large welded structures, welding process often involves multi-pass welding and multi-layer welding etc..The welding sequence of weld seam will have different effects on the quality of the welded structure[4-5]. Therefore, It is very significant for design integrality and the choice of manufacturing process and safety assessment to forecast deformation and residual stress of the welded structure with different welding sequence [6-7].

This study analysis welding sequence and welding deformation of thin-walled and multi-pass welding based on the welding assembly finite element simulation software of ESI Group, PAM-ASSEMBLY. Different welding sequences of a thin-walled structure of Q345D high-strength low-alloy steel (hereafter referred to as Q345D) were numerical simulated. This article describes the qualitative analysis and discussion of contra welding deformation using different programs in order to provide a reference for welding engineering.

II. INTRODUCTION TO PAM-ASSEMBLY

The welding assembly finite element simulation software, PAM-ASSEMBLY, can be highly automated completion of the welding assembly process simulation, allowing designers and manufacturers to quickly simulate thermal deformation due to welding. Users can optimize, compare, and ultimately select the optimal welding sequence and clamp tool[8-9]. This software uses the Local-Global approach when simulating welding assembly. This approach is the most efficient method for large assembly design. In PAM-ASSEMBLY, the Local-Global approach provides a high-level and accurate manufacturing simulation without simplifing the welding physics. In addition, the software has a friendly user interface and uses computation time very efficiently, even for large assemblies.

III. WELDING FINITE ELEMENT MODELING

A. Model meshing.

A visual-mesh is used to establish the finite element model and mesh, as shown in Fig .1. The dimensions of the model are 150mm×90mm×30mm and the thickness of the two steel plates is 0.8mm. Because the model is thin-walled, shell elements may be used for 2D meshing. There are a total of 6526 grid cells.

B. Plate material properties.

In this paper, the material of the plate is Q345D low alloy high strength steel. During software simulation with PAM-ASSEMBLY, the material for simulation chooses steel S355J2G3(The German Steel grade). Steel S355J2G3 according to European standards EN10025-2, working out by ECISS/TC10 'The level and quality of structural steel' technical Committee. Steel S355J2G3 roughly equivalent to Q345D of GB， J2G3 means the heat treatment is normalizing, impact energy of -20℃ is 27J, G3 means deoxy method is FF.

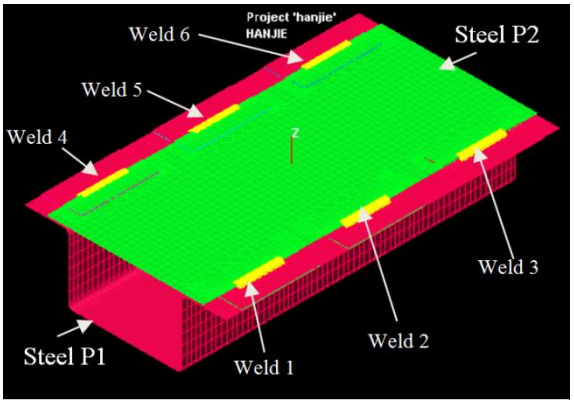

Figure 1. Meshing of the finite element model

As one kind of low alloy and high strength steel, the steel S355J2G3 is main steel material of car beams. In the welding process, welding deformation not only endanger the size tolerance, but also increase the groove gap, let the manufacturing much more difficulty. We need to take some additional procedures to make amends when problems arise, which increase production costs. Take reasonable welding technology can improve the distribution of residual stress state, it is important to improve the service life of the weld structure, the reasonable welding sequence is the key to make welding process.

Because the thermo-physical and mechanical parameters of the material are a function of temperature, temperature plays an important role in the welding simulation and affects the accuracy of the results[10]. The performance parameters of Q345 that change with temperature include the elastic modulus E, the yield strength R_{eL}, the thermal conductivity λ, the linear expansion coefficient α_l, and the specific heat c, as shown in Fig .2.

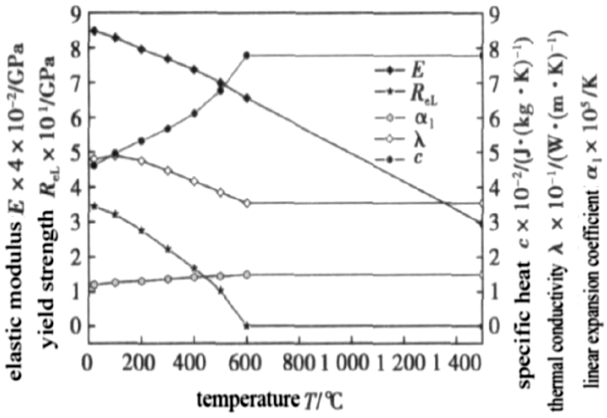

Figure 2. The relationship between mechanical parameters and temperature of Q345[11]

C. *Constraint conditions.*

Eight nodes were defined as constraint points, as shown in Fig .3. The constraint conditions on points 1, 3, 5 and 7 on P2, and points 2, 4, 6 and 8 on P1are shown in Table 1

Shell elements collected in group P1 represent the lower stamped plate of the hat profile assembly. Groups CL2, CL4, CL6 and CL8 (each of them contains one single node) will be used for definition of mechanical boundary conditions for the lower plate P1. Shell elements collected in group P2 represent the upper plate of the hat profile assembly. Groups CL1, CL3, CL5 and CL7 (each of them contains one single node) will be used for definition of mechanical boundary conditions for the upper plate P2.

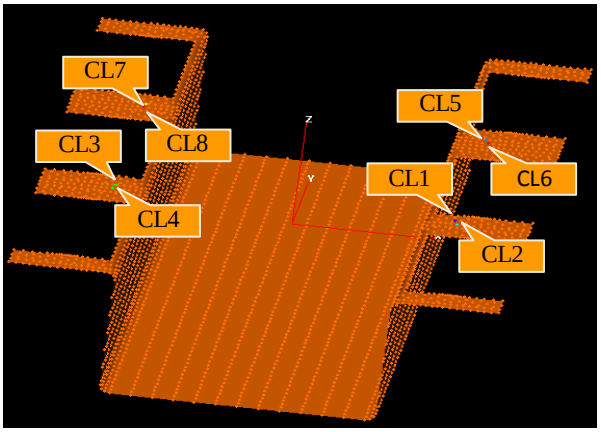

Figure 3. Model of constraint positions

Table 1 Constraint conditions

position	conditions
CL2	UX UY UZ
CL4	UY UZ
CL6	UZ
CL8	UZ
CL1	UX UY UZ
CL3	UY UZ
CL5	UZ
CL7	UZ

IV. WELDING POSITION AND SEQUENCE PROGRAM

A. *Weld position and welding direction.*

The weld position is located in the lap joints of the cover and base frame, and there are a total of six welds, as shown in Fig .4. The blue arrows indicate directions of individual welding trajectories. To reduce the impact of the welding direction of the welding deformation, So try to make reasonable arrangements welding direction. In this article, the welding direction of welds 1, 2, and 4 is along the negative direction of the Y-axis, and the welding direction of welds 3, 5, and 6 is along the positive direction of the Y-axis.

B. *Welding sequence program.*

In this paper, the numerical simulation uses five different welding sequence programs. The specific programs are shown in Table 2.

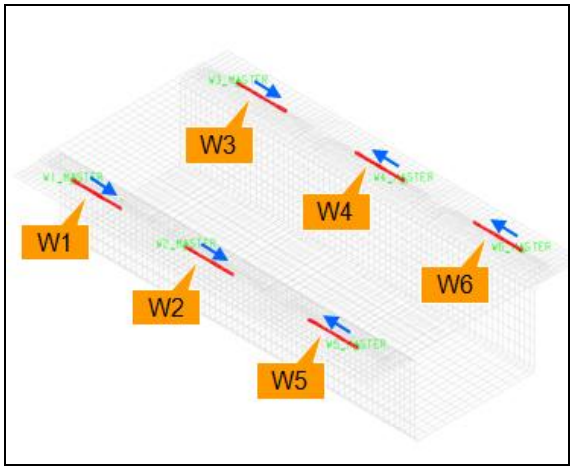

Figure 4. welding direction.

Table 2 Welding sequence for different programs

programs	Welding sequence
1	1—2—3—4—5—6
2	1—4—2—5—3—6
3	1—2—4—5—3—6
4	1—2—4—5—6—3
5	(1-4)—(2-5)—(3-6)

V. THE SIMULATION RESULTS

A. *Welding deformation nephogram.*

After the welding programs 1, 2 and 5 shown in table 2, the whole deformation results are shown in Fig .5(Magnification 8).

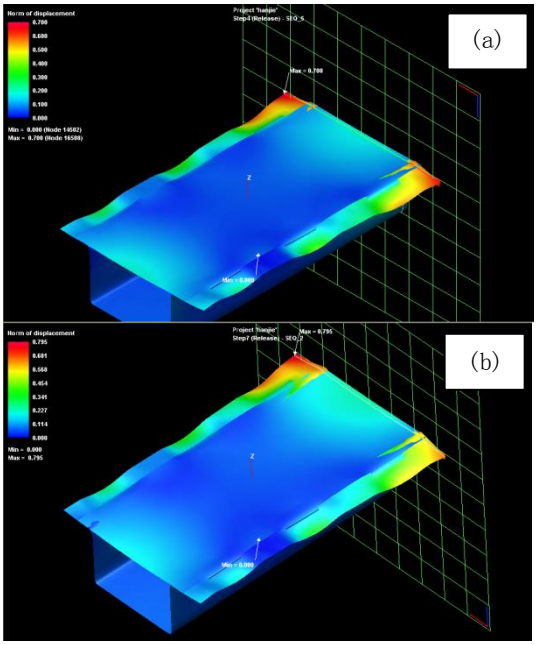

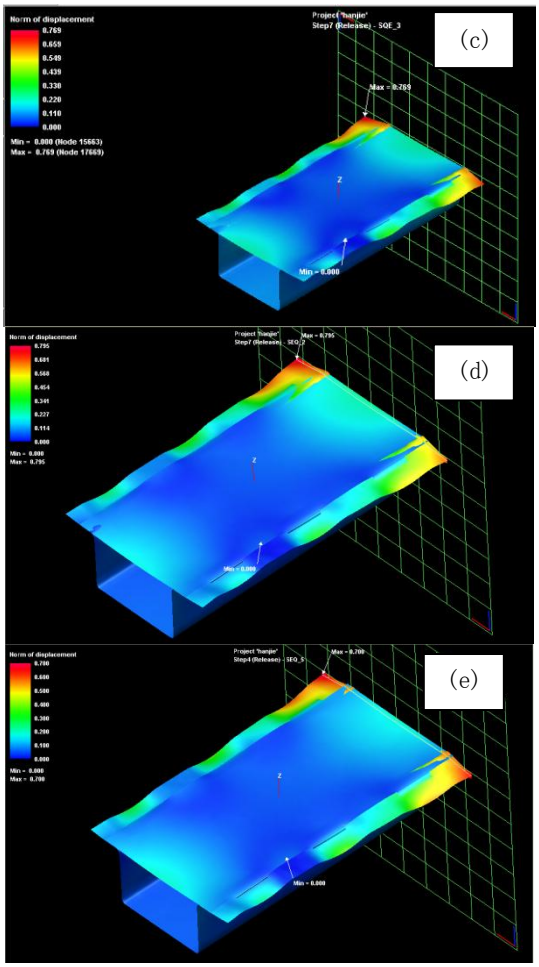

Figure 5. Welding deformation nephograms of different welding programs in table 2 respectively.

These results show that the largest welding deformation is at the top right corner of the model, while the smallest deformation occurs between weld 1 and 2. Because the other parts can freely expand and contract when welding weld 1 and 2, the welding deformation between weld 1 and 2 is smallest. As welding proceeds, heat and deformation will be conducted to the right end of the model. When the welds of the right end of model are finally welded, however, the other welds will have already cooled and cannot freely expand and contract. Therefore, the deformation is largest at the right end of the model.

B. *Analysis and discussion*

A cross-section of the network surface in Fig .4 can be taken to make a graph of the five programs' predicted deformation of each node, as shown in Fig .5.

Throughout the entire model, the maximum deformation is 0.793mm for program 1, 0.795mm for program 2, 0. 792mm for program 3, 0.777mm for program 4, and 0.700mm for program 5.

In program 1, because welds 1, 2, and 3 are welded first , welds 4, 5, and 6 are free to expand and contract. When the next three welds are welded, welds 1, 2, and 3 are cool and cannot freely expand and contract, leading to a greater amount of welding deformation.

Program 2 uses the method of locally symmetric welding, in which the 1, 4 and 2, 6 weld directions are the same. This program results in the maximum amount of welding deformation because the final flexural deformation is partly superimposed.

Program 3 and program 4 have different welding sequences for the last two welds. In program 3, weld 3 is welded before weld 6; in program 4, weld 6 is welded before weld 3. The overall symmetry of the weld sequences of these two programs can effectively offset a portion of the flexural deformation, resulting in a smaller amount of deformation than the first two programs. In program 4, the final weld is weld 3, which occurs after welding of weld 6 and offsets most of the previous flexural deformation. Therefore, program 4 performs better than program 3, as program 4 reduces the deformation relative to program 3 by $(0.792 - 0.777) \div 0.792 \times 100\% = 1.89\%$.

Program 5 uses two short symmetrical seams welded simultaneously, resulting in the minimum welding deformation (0.700 mm), a reduction in deformation between the minimum and maximum of $(0.795 - 0.700) \div 0.795 \times 100\% = 11.95\%$. In this program, both sides of the symmetrical weld are welded at the same time. Thus, the weld's expansion and contraction is isotropic and simultaneous causing reduced deformation because of the constraints on both sides of the weld while welding the first weld and after weld. However, this increases the degree of freedom of the welds, which causes post-weld free expansion along the welding direction. Therefore, the welding sequence causes a smaller welding deformation.

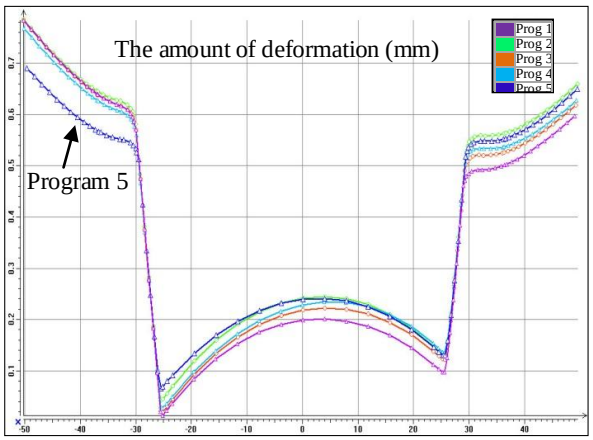

Figure 5. Deformation graph of five programs in table 2 for nodes on this cross-section

VI. CONCLUSION

The following two conclusions can be drawn based on the numerical simulation described in this article.

1) In this article, program 5 reduced the welding deformation by 11.95% compared to program 2, which suggests that reasonable arrangements and assemblages of the welding sequence can effectively reduce the welding deformation.

2) The welding sequence of program 5 resulted in the smallest amount of welding deformation (0.700mm), which suggests that simultaneous welding during actual production is optimal.

ACKNOWLEDGMENT

This work was supported by the National Natural Science Foundation of China (Grant No. 51271158 and No 50975243). This work was also funded by the project of the production-study-research combination of strategic emerging industry of Hunan province.

REFERENCES

[1] X. T. Tian, "Welding Structures," BeiJin: Machinery Industry Press, 2008, pp.72-74.

[2] Z. M. Xue, W.Q. Qu, P. Chai and Y.H. Zhang, "Review on Prediction of Welding Distortion," Transactions of the China Welding Institution, vol. 24, Mar. 2003, pp. 87-90.

[3] S. A. Guo, "Finite Element Prediction of Welding Deformation and Residual Stress in Automotive S355J2G3 Steel I-Beam Welding Structure Under Different Welding Sequences," Working Technology, vol. 42, Jan. 2013, pp 9-13.

[4] T. L. Tong, P. H. Chang and W. C. Tseng, "Effect of Welding Sequences on Residual Stresses," Computer and Structure.vol 81, Mar. 2003, pp. 273-278, doi: 10.1016/S0045-7949(02)00447-9

[5] R. Wang, J.X. Zhang, H. Serizawa avd H. Murakawa, "Study of Welding Inherent Deformations in Thin Plates Based on Finite Doment Analysis Using Interactive Subsmacture Method," Mater. Des., vol. 30, Sept. 2009, pp. 3474-3481, doi: 10.1016/j.matdes. 2009. 03. 015

[6] Y. H. P. Manurung, R. N. Lidam, M. R. Rahim, M. Y. Zakaria, M. R Redza, M. S. Sulaiman, G. Tham and S. K. Abas, "Welding Distortion Analysis of Multipass Joint Combination with Different Sequences Using 3D FEM and Experiment," International Journal of Pressure Vessels and Piping, Vol. 111–112, Jan. 2013, pp. 89-98.

[7] Kiyoshima S, "Quick Welder User's Manual," Research Center of Computatiional Mechanics Inc., Tokyo, 2005, pp. 23.

[8] ESI Group, "SYSWELD 2010 reference manual," Digital Version, 2010.

[9] ESI Group, "SYSWOLD 2010 technical description of capabilities," Digital Version, 2010.

[10] C. S. Wu, "Numerical simulation of welding thermal process," Harbin: Harbin Institute of Technology Press, 1990.

[11] D. J. Yan, X.S. Liu, G.T. Zhou and H.Y. Fang, "Large-scale the backplane structure of welding sequence control deformation Numerical Analysis," Transactions of the China Welding Institution, Vol. 30, Dec. 2009, pp. 55-58.